Communication

# Characterization of a Diferrous Terminal Hydride Mechanistically Relevant to the Fe-Only Hydrogenases

Jarl Ivar van der Vlugt, Thomas B. Rauchfuss, C. Matthew Whaley, and Scott R. Wilson

*J. Am. Chem. Soc.*, **2005**, 127 (46), 16012-16013• DOI: 10.1021/ja055475a • Publication Date (Web): 29 October 2005



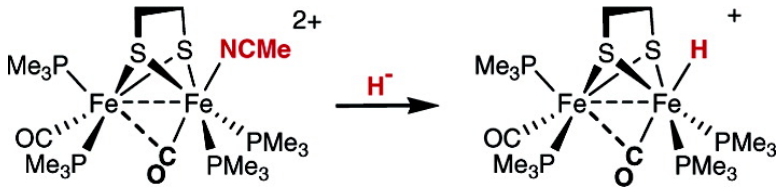


## More About This Article

Additional resources and features associated with this article are available within the HTML version:

- Supporting Information
- Links to the 32 articles that cite this article, as of the time of this article download
- Access to high resolution figures
- Links to articles and content related to this article
- Copyright permission to reproduce figures and/or text from this article

View the Full Text HTML

J|A|C|S
COMMUNICATIONS

Published on Web 10/29/2005

# Characterization of a Diferrous Terminal Hydride Mechanistically Relevant to the Fe-Only Hydrogenases

Jarl Ivar van der Vlugt, Thomas B. Rauchfuss,* C. Matthew Whaley, and Scott R. Wilson

*Department of Chemistry, University of Illinois at Urbana−Champaign, Urbana, Illinois 61801*

Received August 22, 2005; E-mail: rauchfuz@uiuc.edu

Hydrogenases catalyze the formation and oxidation of $H_2$[1] and, as such, are technologically interesting because they utilize base metals and operate at extraordinarily high rates.[2] Of the two structurally characterized classes of hydrogenases, the Fe-only hydrogenases (Fe $H_2$ases)[2] have received intense scrutiny with a focus on both functional and structural modeling.[3,4] Direct insight into the key $H_2$-forming or the $H_2$-binding steps is still lacking, however.

Two functional states of the active site in the Fe $H_2$ases have been characterized (Figure 1). The $H_{ox}$ state ($S = {}^1/_2$) is very likely

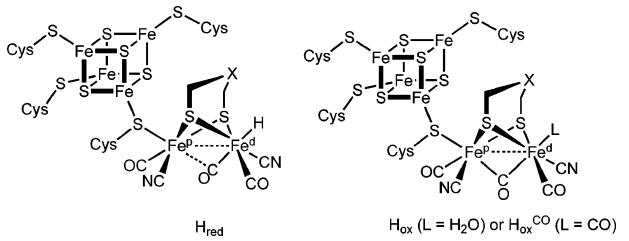


***Figure 1.***

[$Fe^p$(II)$Fe^d$(I)],[5] where $Fe^p$ and $Fe^d$ refer to the Fe center proximal and distal to the attached [4Fe−4S] cluster, respectively. The $H_{red}$ state is diamagnetic, which is consistent with either of two low-spin descriptions: [Fe(II)Fe(II)] or antiferromagnetically coupled (or Fe−Fe bonded) [Fe(I)Fe(I)]. One structural difference between these two functional states is the presence of a symmetrically bridging ($H_{ox}$) or *semi*bridging ($H_{red}$) CO ligand.[6] A second difference is that the axial site on $Fe^d$ is either vacant or occupied by a light atom, such as H in $H_{red}$, whereas $H_2O$ appears to bind at the same site in $H_{ox}$.[7]

Synthetic models of the type $[Fe_2(SR)_2(\mu\text{-H})L_2(CO)_4]^z$ produce $H_2$ by electrocatalytic reduction of protons (L = $CN^-$, $PMe_3$).[8] Such $Fe_2(\mu$-H) species,[9] however, exhibit no inherent reactivity toward protons. Biophysical studies strongly implicate a role for a hydride at the axial site on $Fe^d$; such terminal hydrides are expected to be more hydridic than the isomeric bridging hydrides.[10] *Diferrous species bearing a terminal hydride ligand are unknown, until this report.*[11]

The present study was enabled by our recent synthesis of diferrous dithiolato complexes of the type $[Fe_2(S_2C_nH_{2n})(\mu\text{-CO})(CO)_{5-x}(PR_3)_x(NCMe)]^{2+}$, which contain one substitutionally labile terminal site trans to the Fe−Fe bond.[12] To simplify the spectroscopy, we employ ethanedithiolate ($S_2C_2H_4^{2-}$, $edt^{2-}$) in place of the propane- or azadithiolate cofactor proposed for the enzyme.

Low-temperature reaction of an MeCN solution of $[Fe_2(edt)(\mu\text{-CO})(CO)(PMe_3)_4(NCMe)](PF_6)_2$, [**1**(NCMe)]$(PF_6)_2$, with $LiAlH_4$ or $NaBH_4$ efficiently afforded red $[Fe_2(edt)(\mu\text{-H})(CO)_2(PMe_3)_4]^+$ ([**1**H]$^+$), as confirmed by IR and NMR spectroscopy. For example, the $^1$H NMR spectrum exhibited a triplet-of-triplets at $\delta$ −20.6 ($J_{P-H}$ = 28, 5 Hz).[13] Dark-green $[Fe_2(edt)(\mu\text{-CO})(CO)_2(PMe_3)_3(NCMe)](PF_6)_2$ ([**2**(NCMe)]$(PF_6)_2$) reacted with $LiAlH_4$ to give the analogous hydride, red-colored $[Fe_2(edt)(\mu\text{-H})(CO)_3(PMe_3)_3]PF_6$ ([**2**H]$PF_6$). The $^1$H NMR spectrum of [**2**H]$PF_6$ indicated both minor (∼15%, $\delta$ −15.6, dt) and major isomers ($\delta$ -18.4, ddd). Previously, diferrous hydrides were only accessible via protonation of the Fe−Fe bond in the corresponding di*sub*ferrous $Fe_2(SR)_2L_2(CO)_4$ species.[8]

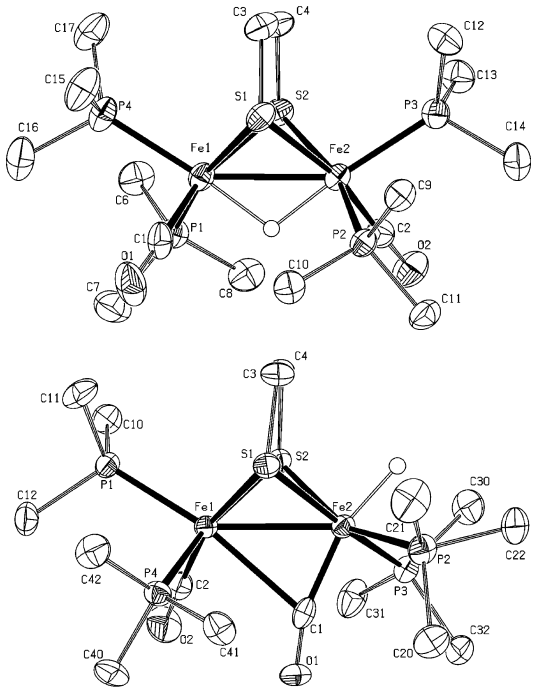


***Figure 2.*** Molecular structure of the monocations in $[Fe_2(edt)(\mu\text{-H})(CO)_2(PMe_3)_4]PF_6$ ([**1**H]$PF_6$) (top) and $[Fe_2(edt)(\mu\text{-CO})(H)(CO)(PMe_3)_4]PF_6$ (α-[**1**H]$PF_6$) (bottom). Displacement ellipsoids are drawn at the 50% probability level. All hydrogen atoms, except the bridging or terminal hydride H(1), are omitted for clarity. [**1**H]$PF_6$ selected bond lengths (Å): Fe(1)−Fe(2) 2.6102(8); Fe(1)−P(1) 2.2330(11); Fe(1)−P(4) 2.2357(12); Fe(2)−P(3) 2.2282(11); Fe(1)−H(1) 1.65(3); Fe(2)−H(1) 1.61(2); Fe(1)−C(1) 1.738-(3); Fe(2)−C(2) 1.754(3); C(1)−O(1) 1.160(3). Angles (°): Fe(2)−Fe(1)−H(1) 36.1(9); Fe(1)−Fe(2)−H(1) 37.3(9); P(1)−Fe(1)−H(1) 87.5(9); P(3)−Fe(2)−H(1) 171.8(9); Fe(2)−Fe(1)−P(1) 109.51(3); Fe(1)−Fe(2)−P(3) 146.69(3); Fe(1)−C(1)−O(1) 176.3(3); Fe(2)−C(2)−O(2) 178.0(3). α-[**1**H]-$PF_6$ selected bond lengths (Å): Fe(1)−Fe(2) 2.5666(7); Fe(1)−C(1) 2.443-(4); Fe(2)−C(1) 1.771(4); Fe(1)−C(2) 1.748(4); Fe(1)−P(1) 2.2129(11); Fe(1)−P(4) 2.2627(11); Fe(2)−P(2) 2.2043(13); Fe(2)−P(3) 2.2173(11); C(1)−O(1) 1.176(4); C(2)−O(2) 1.163(4); Fe(2)−H(1) 1.52(4). Angles (°): Fe(2)−Fe(1)−C(1) 41.31(10); Fe(1)−Fe(2)−C(1) 65.61(12); Fe(1)−C(1)−O(1) 123.2(3); Fe(2)−C(1)−O(1) 163.3(3); P(1)−Fe(1)−C(1) 168.99-(10); P(3)−Fe(2)−C(1) 84.66(12); Fe(2)−Fe(1)−P(1) 147.49(4); Fe(1)−Fe(2)−P(3) 118.31(4); H(1)−Fe(2)−C(1) 162.4(14).

Crystallographic analyses corroborated the molecular structures of $C_2$-symmetric [**1**H]$PF_6$ (Figure 2) and the major isomer of [**2**H]-$PF_6$ (not shown). The stereochemistry in each $\mu$-H derivative differs subtly yet significantly from its precursor;[12] one basal $PMe_3$ ligand



**10.1021/ja055475a CCC: $30.25** 

***Scheme 1***

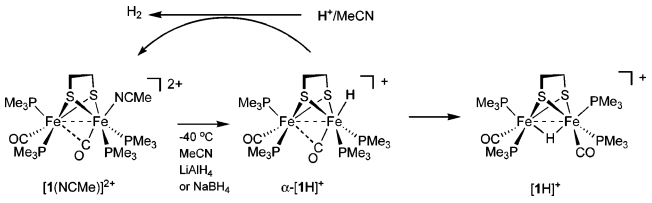


has migrated to the axial position, ostensibly by the migration of a $\mu$-CO ligand, which in turn is displaced by "$H^-$".

The low-temperature (−25 °C) reaction of $LiAlH_4$ or $NaBH_4$ with [**1**(NCMe)]$^{2+}$ in $CD_3CN$ solution revealed a green intermediate, which formed concomitantly with the appearance of free $CH_3CN$ (Scheme 1). This intermediate ($\alpha$-[**1**H]$^+$) exhibited a doublet-of-doublets pattern at $\delta$ −4.6 in the $^1$H NMR spectrum. Low-temperature $^{31}$P−$^1$H HMQC 2D NMR measurements established that this hydride signal is coupled to only two phosphine ligands, at $\delta$ 35.6 ($J_{P-H}$ = 50 Hz) and 21.5 ($J_{P-H}$ = 96 Hz). Using $LiAlD_4$, we prepared $\alpha$-[**1**D]$^+$; selective $^{31}$P{$^1$H}−$^2$H coupling was observed for these two signals, and no hydride signal was found in the $^1$H NMR spectrum. The Fe−H(D) signals were unaffected by $H_2O$ ($D_2O$).

The IR spectrum of $\alpha$-[**1**H]$^+$ featured $\nu_{CO}$ bands at 1940 and 1874 cm$^{-1}$, indicative of both terminal and bridging CO ligands, as well as a weak band at 1844 cm$^{-1}$, attributable to $\nu_{FeH}$ (Figure 3). For $\alpha$-[**1**D]$^+$, the $\nu_{CO}$ bands appeared at 1940 and 1863 cm$^{-1}$.[14]

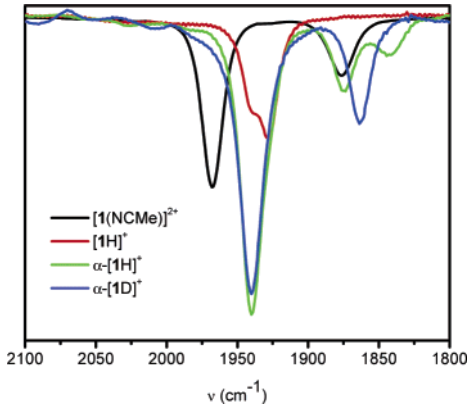


***Figure 3.*** FT-IR spectra (MeCN solution) of [**1**(NCMe)](PF$_6$)$_2$ (black), [**1**H]PF$_6$ (red), $\alpha$-[**1**H]PF$_6$ (green), and $\alpha$-[**1**D]PF$_6$ (blue).

Collectively, the spectroscopic observations support assignment of $\alpha$-[**1**H]$^+$ as the diferrous terminal hydride [Fe$_2$(edt)($\mu$-CO)(H)(CO)(PMe$_3$)$_4$]$^+$. No terminal hydrido intermediate was observed in the reaction of $LiAlH_4$ with [**2**(NCMe)](PF$_6$)$_2$; [**2**H]PF$_6$ formed rapidly even at −25 °C. This result shows that the coligands on the second (proximal, see Figure 1) iron center influence the barrier for the terminal-to-bridging hydride isomerization.

Crystallographic analysis of $\alpha$-[**1**H]PF$_6$ (Figure 2) revealed two independent molecules in the asymmetric unit, each with independently refined terminal hydride ligands. The combination of the terminal hydride, its location trans to the Fe−Fe vector, and the *semi*bridging CO ligand match well with the crystallographic data for the $H_{red}$ form of the enzyme from *D. desulfuricans*. The Fe(1)−C(1) and Fe(2)−C(1) distances of 2.443(4) and 1.771(4) Å, respectively, compare favorably with the corresponding distances of 2.40 and 1.69 Å found for the protein.[6]

The isomerization of $\alpha$-[**1**H]$^+$ to [**1**H]$^+$ was monitored by $^1$H NMR spectroscopy; the process is first order in [$\alpha$-**1**H]$^+$, with $k = 2 \times 10^{-4}$ s$^{-1}$ (21 °C). Other observations indicate that the rearrangement is intramolecular: (i) the rate was unaffected by $H_2O$ or $PMe_3$ (1 equiv); and (ii) isomerization of $\alpha$-[**1**H]PF$_6$ into [**1**H]PF$_6$ also occurred in microcrystalline samples, requiring 2−3 days at room temperature.

Highly relevant to the catalytic function of the Fe-only hydrogenases active site, $CD_2Cl_2$ solutions of $\alpha$-[**1**H]PF$_6$ react at −20 °C (at which temperature the isomerization is slow) with HOTf or H(OEt$_2$)$_2$BAr$^F_4$ to give $H_2$, as confirmed by the $^1$H NMR signal at $\delta$ 4.60. When protonolysis was conducted in the presence of small amounts of MeCN, [**1**(NCMe)]PF$_6$ is regenerated (Scheme 1). Control experiments showed that the corresponding bridging hydride [**1**H]$^+$ is unreactive toward these same acids. Mechanistic studies of the hydrogenogenesis reaction are ongoing.

In summary, reduction of diferrous dithiolates with hydride reagents provides a fresh approach to an active site model for a critically important intermediate. The terminal hydride indeed reacts with Brønsted acids to give $H_2$, in contrast to the *non*reactivity of the isomeric $\mu$-H compounds. The new synthetic methodology could be applicable to other diferrous dithiolates, including those bearing cyanide ligands.[4]

**Acknowledgment.** This research was funded by NIH, DoE, and PRF. We thank Aaron Justice for assistance with the protonation experiments.

**Supporting Information Available:** Preparative, spectroscopic, kinetic, and crystallographic data and methods. This material is available free of charge via the Internet at http://pubs.acs.org.

## References

(1) Frey, M. *ChemBioChem* **2002**, *3*, 153−160.
(2) Cammack, R.; Frey, M.; Robson, R. *Hydrogen as a Fuel: Learning from Nature*; Taylor & Francis: London, 2001.
(3) (a) Tard, C.; Liu, X.; Ibrahim, S. K.; Bruschi, M.; De Gioia, L.; Davies, S. C.; Yang, X.; Wang, L.-S.; Sawers, G.; Pickett, C. J. *Nature* **2005**, *433*, 610−614. (b) Liaw, W.-F.; Tsai, W.-T.; Gau, H.-B.; Lee, C.-M.; Chou, S.-Y.; Chen, W.-Y.; Lee, G.-H. *Inorg. Chem.* **2003**, *42*, 2783−2788.
(4) Boyke, C. A.; van der Vlugt, J. I.; Rauchfuss, T. B.; Wilson, S. R.; Zampella, G.; De Gioia, L. *J. Am. Chem. Soc.* **2005**, *127*, 11010−11018.
(5) Popescu, C. V.; Münck, E. *J. Am. Chem. Soc.* **1999**, *121*, 7877−7884.
(6) Nicolet, Y.; de Lacey, A. L.; Vernede, X.; Fernandez, V. M.; Hatchikian, E. C.; Fontecilla-Camps, J. C. *J. Am. Chem. Soc.* **2001**, *123*, 1596−1601.
(7) Nicolet, Y.; Lemon, B. J.; Fontecilla-Camps, J. C.; Peters, J. W. *Trends Biochem. Sci.* **2000**, *25*, 138−143.
(8) (a) Gloaguen, F.; Lawrence, J. D.; Rauchfuss, T. B. *J. Am. Chem. Soc.* **2001**, *123*, 9476−9477. (b) Mejia-Rodriguez, R.; Chong, D.; Reibenspies, J. H.; Soriaga, M. P.; Darensbourg, M. Y. *J. Am. Chem. Soc.* **2004**, *126*, 12004−12014. (c) Borg, S. J.; Behrsing, T.; Best, S. P.; Razavet, M.; Liu, X.; Pickett, C. J. *J. Am. Chem. Soc.* **2004**, *126*, 16988−16999.
(9) (a) Gloaguen, F.; Lawrence, J. D.; Rauchfuss, T. B.; Bénard, M.; Rohmer, M.-M. *Inorg. Chem.* **2002**, *41*, 6573−6582. (b) Nehring, J. L.; Heinekey, D. M. *Inorg. Chem.* **2003**, *42*, 4288−4292.
(10) Justice, A. K.; Linck, R. C.; Rauchfuss, T. B.; Wilson, S. R. *J. Am. Chem. Soc.* **2004**, *126*, 13214−13215.
(11) A terminal hydride was inferred for a diiron diphosphide system: Cheah, M. H.; Borg, S. J.; Bondin, M. I.; Best, S. P. *Inorg. Chem.* **2004**, *43*, 5635−5644.
(12) van der Vlugt, J. I.; Rauchfuss, T. B.; Wilson, S. R. *Chem.—Eur. J.* **2005**, DOI: 10.1002/chem.200500752.
(13) The larger *J* value is attributed to *cis*-P−H coupling: Zhao, X.; Hsiao, Y.-M.; Lai, C.-H.; Reibenspies, J. H.; Darensbourg, M. Y. *Inorg. Chem.* **2002**, 699−708.
(14) Walker, H. W.; Ford, P. C. *Inorg. Chem.* **1982**, *21*, 2509−2510.

JA055475A